Food Chemistry 241 (2018) 143–149

Contents lists available at ScienceDirect

Food Chemistry

journal homepage: www.elsevier.com/locate/foodchem

Physicochemical and viscoelastic properties of honey from medicinal plants

Huong Thi Lan Nguyen, Naksit Panyoyai, Vilia Darma Paramita, Nitin Mantri, Stefan Kasapis*

School of Science, RMIT University, Bundoora Campus, Bundoora, Vic 3083, Melbourne, Australia

ARTICLE INFO

Keywords:
Honey
Physicochemical properties
Viscoelastic behaviour
Glass transition temperature

ABSTRACT

The present work investigated the physicochemical and structural properties of Tulsi, Alfalfa and two varieties of Manuka honey derived from medicinal plants. Chemical analysis yielded data on the content of reducing sugars (glucose and fructose) that dominate the honey matrix, and of the minor constituents of protein, phenols and flavonoids. Standard chemical assays were used to develop a database of water content, electrical conductivity, pH, ash content, visual appearance and colour intensity. Physicochemical characteristics were related to structural behaviour of the four honey types, as recorded by small-deformation dynamic oscillation in shear, micro- and modulated differential scanning calorimetry, wide angle X-ray diffraction and infrared spectroscopy. The preponderance of hydrogen bonds in intermolecular associations amongst monosaccharides in honey yields a semi-amorphous or semi-crystalline system. That allowed prediction of the calorimetric and mechanical glass transition temperatures that demarcate the passage from liquid-like to solid-like consistency at subzero temperatures.

1. Introduction

Honey is a natural sugar-saturated material used as food sweetener, complete food or medicinal supplement. Epidemiological studies reported protective and therapeutic effects of honey on overall health and well-being by improving the immune, antibacterial and antioxidation response extending to cardiovascular protection (Alvarez-Suarez, Gasparrini, Forbes-Hernández, Mazzoni, & Giampieri, 2014). It is made of sugar, mainly glucose and fructose up to 80% (w/w), and over 180 other components including proteins, free amino acids, essential minerals, vitamins, enzymes and phenolic phytochemicals (Alvarez-Suarez, Giampieri, & Battino, 2013). Phytochemicals are the main source of bioactivity and medicinal properties are transferred to honey through floral nectar and pollen collection by the bees (Alvarez-Suarez et al., 2010). They vary amongst plants to influence the level and diversity of bioactive compounds in honey but phenolic acids and flavonoids are the most abundant.

Tulsi plant (*Ocinum tenuiflorum* L.), Manuka tree (*Leptosperma scoparium*) and Alfalfa plant (*Medicago sativa*) have long been used in Indian traditional medicine as a source of bioactive molecules with therapeutic potential (Bora & Sharma, 2011). Literature reports that their pharmacological effects relate to anticancer, antiinflammation, hypolipidemia and cardioprotection, with the combination of nutritional and prophylactic properties promising long-term health benefits (Upadhyay et al., 2015).

To maximise health benefits and establish a solid platform of analytical information leading to application, there is a need to identify primarily the phenol and flavonoid contents in various types of commercially available honey (Meda, Lamien, Romito, Millogo, & Nacoulma, 2005). Physicochemical characterization including water content, electrical conductivity, ash content, pH, visual colour and colour intensity, reducing sugar, and total protein can facilitate standardisation of honey bee products (Saxena, Gautam, & Sharma, 2010). Furthermore, quality attributes that relate to palatability *via* oral administration and topical treatment for infected wounds require fundamental understanding of the physical state of honey and its thermodynamic transition from liquid to solid-like behaviour as a function of environmental temperature (LeBail et al., 2003).

Honey is a high-solid material and should possess a characteristic glass transition temperature (T_g), which is a parameter widely used to predict, hence optimise the quality and stability of products during processing and subsequent storage. Above the respective T_g value, food products develop a rubbery and/or a melt state, with a considerable decrease in viscosity allowing for greater mobility. This outcome results in structural changes of the condensed matrix including collapse, stickiness, caking and fusion (Santivarangkna, Aschenbrenner, Kulozik, & Foerst, 2011). Below the glass transition temperature, systems enter the glassy region where molecular diffusion, leading to chemical, enzymatic and biological reactions, is limited (Roos, 2010). Recently, the concept of mechanical or network glass transition temperature has been introduced to complement estimates of the calorimetric T_g in glass forming matrices like honey as a function of

* Corresponding author.
E-mail address: stefan.kasapis@rmit.edu.au (S. Kasapis).

http://dx.doi.org/10.1016/j.foodchem.2017.08.070
Received 15 March 2017; Received in revised form 30 June 2017; Accepted 21 August 2017
Available online 24 August 2017
0308-8146/

temperature or timescale of observation (Kasapis, 2006).

Given the above, this study aims to examine the physicochemical and structural properties of various types of honey obtained from different medicinal plants known for antiinflammation and lowering cholesterol properties. Making available information from fundamental studies can facilitate development of product concepts, with honey being the main component, showing an increasingly likelihood of acceptance by the consumer.

2. Materials and methods

2.1. Materials

Four different types of honey, i.e. Tulsi (TUL), Alfafa (ALF) and Manuka (MH1 and MH2), were used in this study. The former is a monofloral honey produced from the nectar of Tulsi plants grown in the green house of RMIT University, Australia. Varieties ALF, MH1 and MH2 are from Pennsylvania (USA), New South Wales (Australia) and Warrandyte (New Zealand), respectively. They were stored in air-tight jars under dark ambient conditions and subjected to 40 °C heating for 5 min to provide a common baseline for all systems prior to experimentation. Chemicals and reagents used in this study were AR standard. Folin–Ciocalteu's phenol reagents (2 N), sodium carbonate (> 99.5%), absolute ethanol (> 99.8%) and gallic acid (> 97.9%) were purchased from Sigma-Aldrich Co (Sydney, Australia).

2.2. Methods

2.2.1. Standard physicochemical analyses

Triplicate measurements were taken from distinct batches for each of the four types of honey studied following the protocol of International Honey Commission (Bogdanov, Martin, & Lullmann, 2002). In doing so, water content and total soluble solids were measured with a Refracto 30GS (Mettler Toledo, Australia) and converted accordingly using the Chetaway Table. Electrical conductivity was measured on SevenCompact Conductivity Meter S230 (Mettler Toledo) at 20 °C in 20% (w/v) honey solution in Milli-Q water. Ash content was obtained by placing 5 g of honey in a crucible (Labec, Australia) and heating at 600 °C overnight in a muffle furnace. pH measurement of 10% (w/v) honey solution was performed following the method of Moniruzzaman, Khalil, Sulaiman, and Gan (2013).

Visual colour was assessed following a method described by Bertoncelj, Doberšek, Jamnik, and Golob (2007). A chromameter CR-400/410 (Konica Minolta, Australia) was used for CIE L^*, a^*, b^* measurements of our samples, where L^*: lightness, $-a^*$: greenness, a^*: redness and b^*: yellowness, as compared with the white tile background. Colour intensity of 50% (w/v) honey solution, which was filtered at 0.45 μm to remove any coarse particles, was measured as described by Beretta, Granata, Ferrero, Orioli, and Maffei Facino (2005). Spectrophotometric absorbance was taken at 450 nm using a Lambda 35 UV–vis spectrophotometer from Perkin Elmer (Waltham, USA).

2.2.2. Reducing sugars

Amounts of D-glucose and D-fructose in honey were determined with Megazyme's Assay Kit (K-SUFRG 06/14). D-glucose was determined by utilising hexokinase and glucose-6-phosphate without hydrolysing sucrose. D-fructose was determined subsequent to the determination of D-glucose following isomerisation with phosphoglucose isomerase. Samples were analysed in triplicate and the mean is expressed as g/100 g honey.

2.2.3. Protein content

This was determined with Thermo Scientific™ Coomassie (Bradford) Protein Assay Kit (23200). Twenty μl of 10% (w/v) honey solution were pipetted into a microplate. Then, 250 μl of Coomassie reagent were added and the plate was put in a shaker to incubate at ambient temperature for 10 min. Absorbance was measured at 595 nm with a Polar microplate reader, against a standard solution of bovine serum albumin (0–100 μg/ml) that reached linearity of $R^2 = 0.994$. Milli-Q water was used as blank, and each sample was analysed in triplicate, with the mean being expressed in mg/100 g honey.

2.2.4. Total phenolic content

This was determined with the Folin-Ciocalteu method (Singleton, Orthofer, & Lamuela-Raventós, 1999). Honey sample (5 g) was diluted to 50 ml with Milli-Q water and filtered through Whatman No. 1 paper. Solution (0.5 ml) was mixed with 2.5 ml of 0.2 N Folin-Ciocalteu reagent (Sigma-Aldrich, Australia) for 5 min and 2 ml of 75 g/l sodium carbonate was then added. Mixture was incubated at ambient temperature for 2 h before reading with a Lambda 35 UV–vis spectrophotometer. Absorbance was measured at 760 nm against an ethanol blank. Gallic acid was used to produce a standard curve from 0 to 100 mg/l and obtained linearity was $R^2 = 0.999$. All analyses were carried out in triplicate and the mean was expressed in mg of gallic acid equivalents (GAE)/100 g honey.

2.2.5. Fourier transform infrared spectroscopy

A spectrometer equipped with a MIRacleTM ZnSe single reflection ATR plate (Perkin-Elmer, Norwalk, USA) was used to record FTIR spectra for honey. In doing so, 0.5 g was placed onto the measuring plate and scanned forty times from 4000 to 650 cm^{-1} at a resolution of 4 cm^{-1} at ambient temperature.

2.2.6. X-ray diffraction analysis

Presence of crystal nuclei in honey was examined using a D4 Advanced Bruker AXS (Karlsruhe, Germany) attached with a Cu-Kα radiation source (l = 1.54 A°). Triplicate samples were loaded onto the measuring holder and covered with an X-ray film. Raw data were obtained within a 2θ range of 5–90° in the interval of 0.1° and subsequently analysed using Diffract.EVA version 4.1.1.

2.2.7. Modulated and microdifferential scanning calorimetry

First-order thermodynamic transitions of honey were detected with a Setaram VII microdifferential scanning calorimeter (Seturau, France). Hundred mg of honey were loaded into a standard Hastelloy cell and an identical-weight water sample was used as reference. They were equilibrated for 20 min at 20 °C, heated to 90 °C, and then cooled to 20 °C at 1 °C/min. Heat capacity measurements to determine the calorimetric glass transition temperature were conducted on Q2000 calorimeter (TA instruments, New Castle, USA), with nitrogen purge gas at a flow rate of 50 ml/min. Ten mg of honey were loaded into a hermetic aluminium pan and equilibrated for 20 min at 20 °C. Samples were cooled to −90 °C and heated up to 30 °C at 1 °C/min. Triplicate measurements were performed at modulation amplitude of 0.53 °C every 40 s.

2.2.8. Viscoelastic analysis

This was performed with ARG-2 controlled strain rheometer using a magnetic-thrust bearing technology (TA Instruments, New Castle, USA). The rheometer was connected to a liquid nitrogen system to achieve rapid and uniform cooling. Parallel plates of 5 mm diameter and 1 mm gap were used, with samples (0.5 g) being loaded at 15 °C and covered with silicone oil (BDH; 50 cS) to minimise moisture loss. They were equilibrated at 15 °C for 10 min, then cooled deeply within the subzero regime at 1 °C/min with a frequency of 1 rad/s and strain of 0.01%. Frequency sweeps of 0.1 to 100 rad/s were taken from −60 to −20 °C at intervals of three degree centigrade. Time-temperature superposition principle was implemented to generate the master curve of viscoelasticity for honey.

2.2.9. Statistical analysis

Statistical differences in Table 1, represented by letters in the same row for the physicochemical properties of all samples, were obtained

Table 1
Characteristic parameters of honey.

	TUL	ALF	MH1	MH2
Physicochemical parameters				
Water content (%)	18.7 ± 0.3b	18.2 ± 0.3a	18.5 ± 0.1ab	19.1 ± 0.2c
Electrical conductivity (μS/cm)	0.80 ± 0.01d	0.16 ± 0.01a	0.54 ± 0.01c	0.44 ± 0.01b
Ash content (%)	0.16 ± 0.01c	0.04 ± 0.01a	0.11 ± 0.05b	0.07 ± 0.01ab
pH	4.1 ± 0.1b	3.9 ± 0.1a	4.1 ± 0.1b	4.0 ± 0.1a
Visual colour				
L^*	66.9 ± 0.4c	44.2 ± 1.6b	47.8 ± 0.5b	32.5 ± 2.50a
a^*	−4.1 ± 0.1a	−2.0 ± 0.1b	12.9 ± 0.4d	3.1 ± 1.2c
b^*	26.8 ± 1.2c	7.7 ± 0.3a	36.3 ± 1.3d	16.9 ± 1.6b
Colour intensity (mAU)	743 ± 3b	174 ± 1a	2201 ± 60d	1574 ± 8c
Reducing sugars (g/100 g honey)				
Glucose	34.9 ± 3.4b	30.9 ± 3ab	28.9 ± 2a	29.9 ± 0.3ab
Fructose	38.3 ± 3a	36.4 ± 2a	44.2 ± 2b	37.4 ± 0.6a
Total protein (mg/100 g honey)	147.1 ± 5d	102.9 ± 3a	128.5 ± 1c	117.6 ± 2b
Total phenol (mg GAE/100 g honey)	50.6 ± 2.7b	18.3 ± 0.3a	72.1 ± 2c	75.4 ± 0.8c
Total flavonoid (mg QE/100 g honey)	3.74 ± 0.08b	1.92 ± 0.12a	9.57 ± 0.16d	6.46 ± 0.09c
Viscoelastic parameters				
T_g (°C)	−47	−45	−44	−46
C_1^g	10.70	10.85	11.43	11.13
C_2^g (deg)	50	50	50	50
f_g	0.040	0.040	0.038	0.038
α_f (deg^{-1})	8.0×10^{-4}	8.0×10^{-4}	7.6×10^{-4}	7.6×10^{-4}
E_a (kJ/mol)	108	86	81	99

Note: 1. Data are mean ± STD of triplicate measurements taken from distinct batches for each of the four types of honey studied, with different letters in the same row (a–d) indicating significant differences ($p < 0.05$) using Duncan's multiple-range test.
2. TUL = Tulsi honey, ALF = Alfafa honey, MH1 = Manuka honey 1 having unique Manuka factor 20+, and MH2 = Manuka honey 2 having methylglyoxal 400+.

through one-way analysis of variance (ANOVA). This was followed by Duncan's multiple-range test with $p < 0.05$, and it was run on SPSS version 22 (IBM Australia Limited, NSW).

3. Results and discussion

3.1. Quality parameters characterising honey

A plethora of physicochemical and viscoelastic parameters have been obtained for the various types of honey in this investigation and these have been summarised in Table 1. To start with, water content for all samples remained within the range of 18.6 ± 0.5%, i.e. below 20% (w/w), which is the limit approved by the European Union (number 110; EEC, 2001) and similar to that found earlier (Habib, Al Meqbali, Kamal, Souka, & Ibrahim, 2014). This is an important quality criterion indicating shelf-life and ripeness, with high water content promoting fermentation of honey by osmotolerant yeasts. Electrical conductivity varies from about 0.16 to 0.80 μS/cm. Honey contains organic acids and mineral salts, which are chemically ionizable and conduct electric current in solution, and this is affected by botanical origin. Based on European Union guidelines, it should not exceed 0.8 μS/cm for nectar flower honey, which is a determinant of good quality with the exception of some plant species such as strawberry tree (*Arbutus unedo*), bell heather (*Erica*), etc.

Ash content analysis represents the level of minerals and trace elements, and yields values between 0.07 and 0.16%, with TUL being at the upper end of the range (Table 1). Correlation coefficient between electrical conductivity and ash content is very good ($R^2 = 0.810$) in the present study. Ash values are within the limit allowed for blossom honey (≤0.6%) indicating clearness and no adulteration with molasses (EEC, 2001). Nectar honey contains minerals from 0.1 to 0.3% while honeydew honey can reach 1.0% of the total (Belay et al., 2017; Bogdanov, 2009). pH measurements indicate that our honey samples are acidic within normal expectations being comparable to the previous findings of 3.5–4.7 (Saxena et al., 2010). Visual appearance of honey was characterised by a set of tristimulus values arguing that the Tulsi honey possesses the lightest colour ($L^* = 66.9$) with a blend of yellowish and greenish hues. Its colour intensity in the form of absorbance at 450 nm was intermediate (743.2 mAU) between ALF (174.5 mAU) and MH1 (2201.5 mAU), an outcome which is congruent with earlier observations for several types of honey ranging from 125 to 3400 mAU (Beretta et al., 2005; Habib et al., 2014).

The overall content of reducing sugar (glucose and fructose) shown in Table 1 is similar amongst the honey varieties examined presently demarcating a range of 70 ± 3% solids, an outcome which is in line with previous observations (Gomes, Dias, Moreira, Rodrigues, & Estevinho, 2010; Habib et al., 2014). However, the individual amounts of D-glucose and D-fructose in TUL (34.9 and 38.3 g, respectively) is statistically distinct from those in MH1 (28.9 and 44.2 g, respectively). The ratio of fructose-to-glucose indicates the physical state of the honey matrix, and when this is less than 1.0, it crystallises rapidly (Draiaia et al., 2015). Total protein content was determined with bovine serum albumin as the standard and, accordingly, it makes our samples fall into the category of "high protein" honey compared to the range of 41 to 79 mg/100 g reported in the literature (Kishore, Halim, Syazana, & Sirajudeen, 2011). Protein in honey is mainly composed of enzymes or amino acids varying with floral source, enzymes from the honeybees and nectar, and length of storage (Saxena et al., 2010).

Total phenol and flavonoid content in TUL was higher than ALF but lower than MH1 and MH2. Results match those of visual appearance reported in Table 1, where honey with a stronger colour intensity exhibits a higher phytochemical content. Since phenolic content is strongly correlated with antioxidant activity (Mahmoodi-Khaledi et al., 2017; Meda et al., 2005), this parameter is a good criterion for a quick assessment of honey bioavailability.

3.2. Physicochemical characterization of honey

Building a database of quality parameters allowed us to further examine the samples of this investigation by subjecting them to a chemometric analysis based on Fourier transform infrared spectroscopy, wide-angle X-ray diffraction, and microdifferential scanning calorimetry. Fig. 1 illustrates vibrational assignments corresponding to specific chemical linkages obtained using FTIR. Broad bands in 3700–3000 cm^{-1} and 3000–2800 cm^{-1} regions correspond to O–H stretching, indicating the presence of bound and free water molecules,

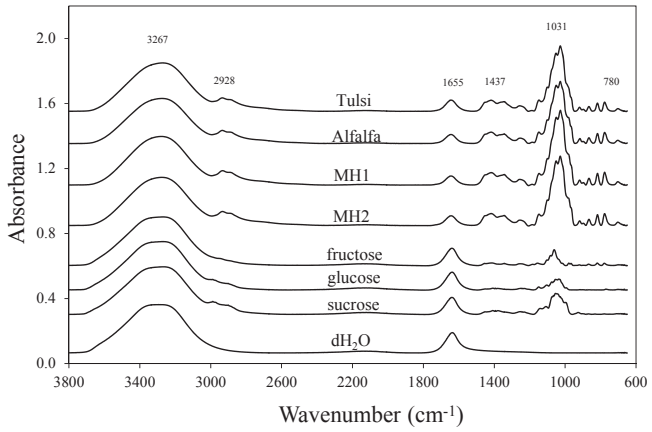

Fig. 1. FTIR spectra of Tulsi, Alfalfa, MH1 and MH2 honey, condensed fructose, glucose and sucrose systems at a moisture content of 19% (w/w), and distilled water.

and C–H stretching of sugars present in honey (Tewari & Irudayaraj, 2004). Infrared vibrations appearing in 1540–1175 cm^{-1} are specific of bending modes for C–C–H, C–O–H and O–C–H groups (Pataca, Neto, Marcucci, & Poppi, 2007).

There is a significant absorbance band in 1175–940 cm^{-1} primarily from C–O and C–C stretching modes, which makes this region a suitable fingerprint for assessment of honey's sugars (Anjos, Campos, Ruiz, & Antunes, 2015). Bands in 900–750 cm^{-1} arose primarily from specific saccharide configurations of C–O and C–C stretching modes being relatively intense in the various types of honey examined here but not in fructose, glucose or sucrose molecules. Finally, a peak at 1655 cm^{-1} appearing in all samples (including distilled water) is due to bending of H–O–H molecules.

Next, we assessed the morphological characteristics of our samples using WAXD (Fig. 2). TUL and MH1 exhibit an amorphous structure, as for the concentrated fructose preparations, with a typical broad peak occurring at ~20°. From MH2 to ALF there is an increasing number of peaks, which indicate crystallinity in honey similar to that recorded for pure sucrose and glucose systems. A peak at 44° being specific to all samples but MH1 is suggestive of aliphatic carbon chains (Paramita, Bannikova, & Kasapis, 2015).

Thermal analysis was conducted on micro-DSC at a scan rate of 1 °C/min for the samples of this investigation (Fig. 3). Upon heating, maxima in endothermic peaks were observed at about 47 and 50 °C for MH2 and ALF, respectively, which were similar in overall shape arguing

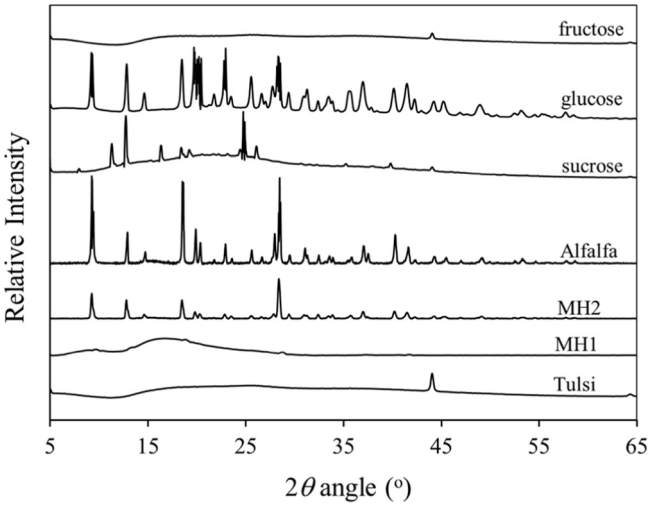

Fig. 2. X-ray diffractograms of fructose, glucose and sucrose systems at a moisture content of 21% (w/w), and Alfalfa, MH2, MH1 and Tulsi honey.

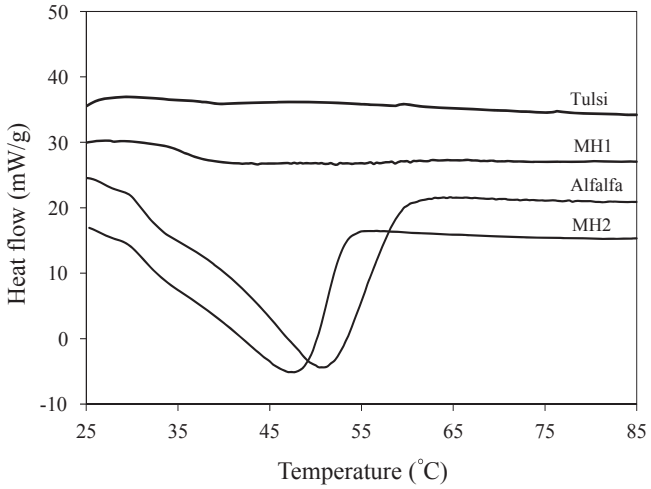

Fig. 3. MicroDSC heating profiles for Tulsi, MH1, Alfalfa and MH2 honey at a scan rate of 1 °C/min.

for a single molecular process. In contrast, TUL and MH1 appeared in essence as featureless thermograms. Endothermic events should be due to the melting of sugar crystals in the honey matrix, an event that depends on sample composition and storage conditions. Results are congruent with the X-ray diffractograms in Fig. 2, which produced largely flat baselines in TUL and MH1, but multiple peak spectra in MH2 and ALF.

3.3. Determination of the calorimetric glass transition temperature for honey

Besides the first-order thermodynamic transition recorded for some honey samples in the preceding section, high-solid systems should also exhibit an element of vitrification upon controlled cooling. This is best related to the glass transition region, which has been monitored presently well into the subzero regime (Fig. 4). A step change of heat capacity is observed for all systems with heating from −75 to −15 °C, an outcome which indicates a devitrification process. The onset, midpoint and endset temperatures have been considered as empirical indicators of the calorimetric glass transition temperature and, in general, this depends on parameters including solids level, sample annealing and scan rate to mention but a few. The four types of honey in our study exhibited a midpoint T_g of −47 ± 2 °C being in good agreement with previous estimates that range from −47 to −51 °C (Ahmed, Prabhu,

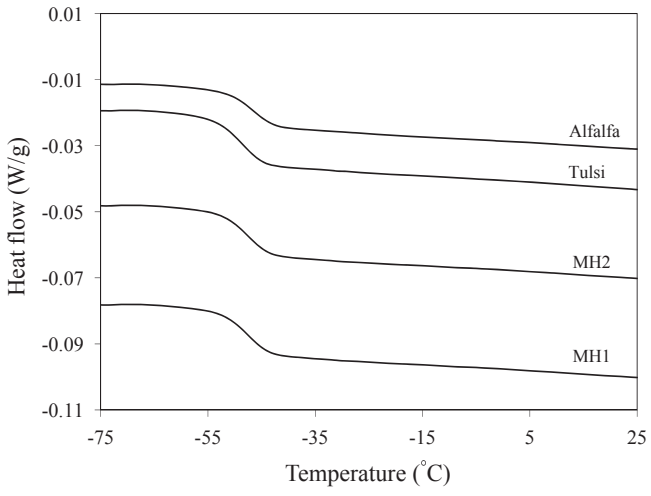

Fig. 4. Modulated DSC heating profiles of Alfalfa, Tulsi, MH2 and MH1 honey at a scan rate of 1 °C/min.

Raghavan, & Ngadi, 2007).

The magnitude and temperature band of the thermal transition for honey is mainly influenced by the plasticizing effect of water content, which is about 18.5% as highlighted in Table 1. That should also be affected by the chemical composition of glucose, fructose, protein, pigments and other solid constituents (Cordella et al., 2002). A previous study on polysaccharide/sugar systems reported a fifty centigrade depression of the calorimetric T_g values as a result of water plasticization from 10 to 20%, w/w (Roos & Karel, 1991). The nature of calorimetric measurements reflects primarily the sugar content, as opposed to molecular interactions between structural components of the high-solid matrix. Mechanical spectroscopy, on the other hand, is ideally posed to examine such interactions supporting long range effects in relation to predictions of the glass transition temperature, and this will be dealt with next.

3.4. Determination of the mechanical glass transition temperature for honey

Viscoelastic properties were evaluated with dynamic oscillatory measurements in-shear yielding values of storage modulus (G') and loss modulus (G'') that reflect the relative solid-like and liquid-like properties of materials (Panyoyai, Bannikova, Small, & Kasapis, 2015). Fig. 5a depicts the variation in values of G' and G'' for Tulsi honey with controlled cooling at 1 °C/min. There is a sharp increase in moduli of four orders of magnitude from 10^5 to 10^9 Pa with cooling at subzero temperatures. This is known as the glass transition region where the viscous component dominates over the elastic component of the system. At the low end of the temperature range, modulus traces crossover to yield a dominant elastic response, and remain essentially constant. This is known as the glassy state where long-range molecular movements, hence physicochemical reactions are limited.

To advance the discussion from a qualitative to a quantitative treatment that deconvolutes the temperature and time contributions to the viscoelastic spectrum, we employed the time-temperature superposition principle (Kasapis, Al-Marhoobi, & Mitchell, 2003). In doing so, we implemented a series of frequency sweeps from 0.1 to 100 rad/s at constant temperature intervals of three degree centigrade. Fig. 5b reproduces data for storage modulus in Tulsi, which remain unchanged in the glassy state (e.g. −54 °C) but show a strong frequency dependence in the glass transition region (e.g. −24 °C); G'' data for Tulsi is not plotted here.

Mechanical spectra of storage and loss modulus were superposed horizontally by selecting an arbitrary reference temperature in the glass transition region ($T_o = -42$°C) and shifting the remainder left or right in relation to T_o in order to generate the master curve of viscoelasticity for Tulsi honey (Fig. 5c). This reproduced the passage of viscoelastic functions from the glass transition region to the glassy state over a wide frequency range, i.e. $10^{-3.5}$–$10^{3.5}$ rad/s, and represents the time (or frequency) analogue of the temperature profile discussed in Fig. 5a.

Horizontal superposition of frequency sweeps to construct the viscoelastic master curve generates a set of shift factors, a_T, which constitute a fundamental mechanism in honey vitrification. These are plotted against experimental temperature in Fig. 5d for TUL (and also MH1) honey. Within the temperature range of the glassy state, there is a linear correlation between temperature and log a_T suggesting that solidified honey follows the predictions of the reaction rate theory, as

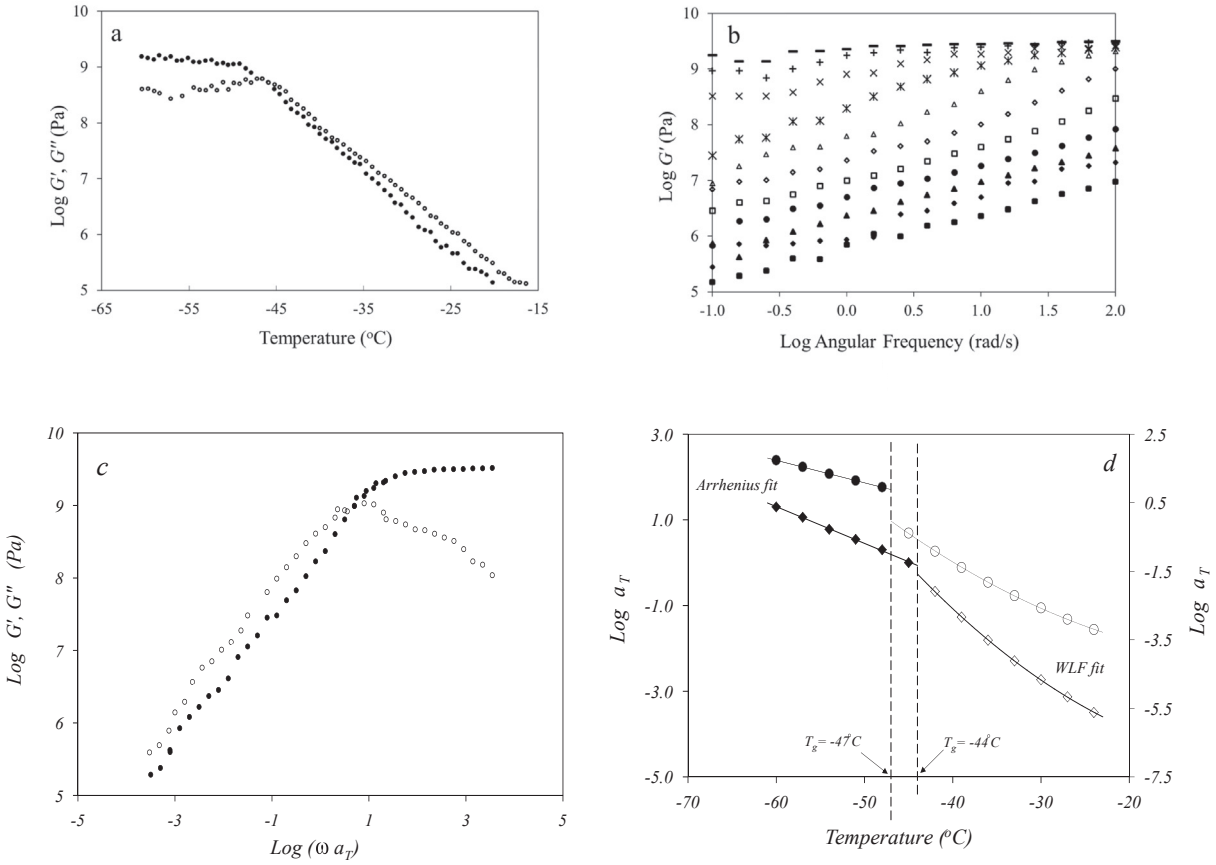

Fig. 5. (a) Heating profiles of G' (●) and G'' (○) for Tulsi honey at a rate of 1 °C/min, frequency of 1 rad/s and strain of 0.01%, (b) Frequency variation of G' for Tulsi honey at −54(–), −51(+), −48(×), −45(*), −42(△), −39(◇), −36(□), −33(●), −30(▲), −27 (♦) and −24(■) °C arranged successively downwards, (c) Master curve of viscoelasticity for reduced shear modulus (G'_p, ● and G''_p, ○) for Tulsi honey, and (d) Shift factors as a function of experimental temperature for Tulsi (●,○; right y-axis) and MH1 (♦,◇; left y-axis) honey with the Arrhenius fit (close symbols) and WLF fit (open symbols); dashed lines pinpoint predictions of the mechanical T_g.

described by the modified Arrhenius equation (Kasapis, 2008):

$$\log a_T = \frac{E_a}{2.303R}\left(\frac{1}{T} - \frac{1}{T_\circ}\right) \quad (1)$$

where, E_a is the activation energy for permitted vibrations from one conformational state to another and R is the universal gas constant. E_a values are calculated to be ~108 and 81 kJ/mol for TUL and MH1, respectively, and similar estimates are cited for ALF and MH2 in Table 1. The above energy of activation values afford direct comparison of molecular dynamics between carbohydrate matrices with glassy consistency. They are comparable to glucose syrup and glucose syrup/K-carrageenan systems at 80% (w/w) solids (98 and 140 kJ/mol) used as excipients for bioactive compound encapsulation (Kasapis & Shrinivas, 2010). However, the energy of activation of bioactive compounds (e.g. caffeine) is considerably lower (0.23–0.47 kJ/mol) reflecting the freedom of caffeine to diffuse within the glassy carbohydrate matrix.

At the upper temperature range of the glass transition, progress in viscoelasticity for TUL and MH1 is better described in Fig. 5d by the theoretical framework of free volume, as modelled by the Williams, Landel and Ferry equation (Ferry, 1980):

$$\log a_T = -\frac{C_1^0(T-T_0)}{C_2^0 + T - T_0} = -\frac{(B/2.303f_0)(T-T_0)}{(f_0/\alpha_f) + T - T_0} \quad (2)$$

where $C_1{}^0$ and $C_2{}^0$ are the WLF constants at $T_\circ$ ($C_1{}^g$ and $C_2{}^g$ at T_g), $f_\circ$ is the fractional free volume at T_o (f_g at T_g), α_f is the thermal expansion coefficient (deg^{-1}) above T_g, and B is usually set to 1.

Data fitting to the WLF model was also implemented for ALF and MH2 and results are summarised in Table 1. As far as we are aware, values of WLF constants, fractional free volume, thermal expansion coefficient and mechanical T_g, based on free volume theory, are given for the first time in honey systems. These are according to experience for amorphous synthetic polymers and condensed carbohydrate matrices undergoing glass transition (Kasapis, 2008). Estimates of the fractional free volume at the glass transition temperature are about 0.040 indicating that the honey matrix has reached a state of kinetically trapped equilibrium in molecular relaxation (Roos, 2010).

Values of the mechanical glass transition temperature range between −44 and −47 °C for the various types of honey in this investigation. They are comparable to the estimates from calorimetric T_g in Fig. 4 recorded at about −47 °C from the midpoint of the sigmoidal thermograms. In both cases, honey samples were identical in terms of composition and preparation history, and in the absence of three-dimensional polymeric structures, it is the sugar molecules that determine the vitrification patterns for both analytical techniques.

4. Conclusions

The present investigation develops a detailed picture of the physicochemical and viscoelastic properties of four types of honey, i.e. Tulsi, Alfalfa and two types of Manuka, from medicinal plants. Quality criteria are in accordance with the international regulations from the European Union for good quality honey. This includes the relatively high total phenolic and flavonoid content that supports a potential for natural remedy. Results indicate that at ambient temperature honey is a supercooled liquid with glucose crystals being precipitated into a solution of fructose and other minor ingredients. Therefore, MH1 and TUL honey with a relatively-high fructose content produce amorphous diffractograms (as for the pure fructose sample) shown in Fig. 2, and flat microDSC thermograms shown in Fig. 3. In contrast, ALF and MH2 honey exhibit multiple WAXD peaks whose glucose crystals liquefy in an endothermic transition recorded calorimetrically. Condensed systems of polysaccharide/sugar or protein/sugar yield different predictions for the mechanical and DSC T_g, due to the distinct property and distance scale being probed by the two techniques. In the absence of polymeric network formation in honey, however, thermomechanical predictions of glass transition temperature coincide, hence emphasizing the predominant role of bulky sugars in the metastable state of honey matrix. Finally, successful utilisation of the WLF equation in this work allowed estimation of the free volume parameters for honey vitrification.

Acknowledgments

PhD scholarship to Huong Thi Lan Nguyen by VIED and RMIT is duly acknowledged.

References

Ahmed, J., Prabhu, S., Raghavan, G., & Ngadi, M. (2007). Physico-chemical, rheological, calorimetric and dielectric behaviour of selected Indian honey. *Journal of Food Engineering, 79*, 1207–1213.

Alvarez-Suarez, J. M., Gasparrini, M., Forbes-Hernández, T. Y., Mazzoni, L., & Giampieri, F. (2014). The composition and biological activity of honey: A focus on Manuka honey. *Foods, 3*(3), 420–432.

Alvarez-Suarez, J. M., Giampieri, F., & Battino, M. (2013). Honey as a source of dietary antioxidants: Structures, bioavailability and evidence of protective effects against human chronic diseases. *Current Medicinal Chemistry, 20*, 621–638.

Alvarez-Suarez, J. M., Tulipani, S., Díaz, D., Estevez, Y., Romandini, S., Giampieri, F., & Battino, M. (2010). Antioxidant and antimicrobial capacity of several monofloral Cuban honeys and their correlation with color, polyphenol content and other chemical compounds. *Food and Chemical Toxicology, 48*, 2490–2499.

Anjos, O., Campos, M. G., Ruiz, P. C., & Antunes, P. (2015). Application of FTIR-ATR spectroscopy to the quantification of sugar in honey. *Food Chemistry, 169*, 218–223.

Belay, A., Haki, G. D., Birringer, M., Borck, H., Lee, Y. C., Cho, C. W., ... Melaku, S. (2017). Sugar profile and physicochemical properties of Ethiopian monofloral honey. *International Journal of Food Properties*. http://dx.doi.org/10.1080/10942912.2016.1255898.

Beretta, G., Granata, P., Ferrero, M., Orioli, M., & Maffei Facino, R. (2005). Standardization of antioxidant properties of honey by a combination of spectrophotometric/fluorimetric assays and chemometrics. *Analytica Chimica Acta, 533*, 185–191.

Bertoncelj, J., Doberšek, U., Jamnik, M., & Golob, T. (2007). Evaluation of the phenolic content, antioxidant activity and colour of Slovenian honey. *Food Chemistry, 105*, 822–828.

Bogdanov, S. (2009). The book of honey. Bee product science. Available at www.bee-hexagon.net.

Bogdanov, S., Martin, P., & Lullmann, C. (2002). *Harmonised methods of the international honey commission.* Liebefeld: Swiss Bee Research Centre FAM.

Bora, K. S., & Sharma, A. (2011). Phytochemical and pharmacological potential of Medicago sativa: A review. *Pharmaceutical Biology, 49*, 211–220.

Cordella, C., Antinelli, J.-F., Aurieres, C., Faucon, J.-P., Cabrol-Bass, D., & Sbirrazzuoli, N. (2002). Use of differential scanning calorimetry (DSC) as a new technique for detection of adulteration in honeys. 1. Study of adulteration effect on honey thermal behavior. *Journal of Agricultural and Food Chemistry, 50*, 203–208.

Draiaia, R., Dainese, N., Borin, A., Manzinello, C., Gallina, A., & Mutinelli, F. (2015). Physicochemical parameters and antibiotics residuals in Algerian honey. *African Journal of Biotechnology, 14*, 1242–1251.

European Economic Community (EEC) (2001). Composition criteria for honey. Council directive 2001/110/EC Annex II. *Official Journal of the European Communities, L10*, 47–52.

Ferry, J. D. (1980). *Viscoelastic properties of polymers.* John Wiley & Sons.

Gomes, S., Dias, L. G., Moreira, L. L., Rodrigues, P., & Estevinho, L. (2010). Physicochemical, microbiological and antimicrobial properties of commercial honeys from Portugal. *Food and Chemical Toxicology, 48*, 544–548.

Habib, H. M., Al Meqbali, F. T., Kamal, H., Souka, U. D., & Ibrahim, W. H. (2014). Physicochemical and biochemical properties of honeys from arid regions. *Food Chemistry, 153*, 35–43.

Kasapis, S. (2006). Definition and applications of the network glass transition temperature. *Food Hydrocolloids, 20*, 218–228.

Kasapis, S. (2008). Recent advances and future challenges in the explanation and exploitation of the network glass transition of high sugar/biopolymer mixtures. *Critical Reviews in Food Science and Nutrition, 48*, 185–203.

Kasapis, S., Al-Marhoobi, I. M., & Mitchell, J. R. (2003). Testing the validity of comparisons between the rheological and the calorimetric glass transition temperatures. *Carbohydrate Research, 338*, 787–794.

Kasapis, S., & Shrinivas, P. (2010). Combined use of thermodynamics and UV spectroscopy to rationalize the kinetics of bioactive-compound (caffeine) mobility in a high solids matrix. *Journal of Agricultural and Food Chemistry, 58*, 3825–3832.

Kishore, R. K., Halim, A. S., Syazana, M. N., & Sirajudeen, K. (2011). Tualang honey has higher phenolic content and greater radical scavenging activity compared with other honey sources. *Nutrition Research, 31*, 322–325.

LeBail, A., Boillereaux, L., Davenel, A., Hayert, M., Lucas, T., & Monteau, J. Y. (2003). Phase transition in foods: Effect of pressure and methods to assess or control phase transition. *Innovative Food Science and Emerging Technologies, 4*, 15–24.

Mahmoodi-Khaledi, E., Lozano-Sánchez, J., Bakhouche, A., Habibi-Rezaei, M., Sadeghian,

I., & Segura-Carretero, A. (2017). Physicochemical properties and biological activities of honeys from different geographical and botanical origins in Iran. *European Food Research and Technology, 243*, 1019–1030.
Meda, A., Lamien, C. E., Romito, M., Millogo, J., & Nacoulma, O. G. (2005). Determination of the total phenolic, flavonoid and proline contents in Burkina Fasan honey, as well as their radical scavenging activity. *Food Chemistry, 91*, 571–577.
Moniruzzaman, M., Khalil, M. I., Sulaiman, S. A., & Gan, S. H. (2013). Physicochemical and antioxidant properties of Malaysian honeys produced by *Apis cerana*, *Apis dorsata* and *Apis mellifera*. *BMC Complementary and Alternative Medicine, 13*, 43.
Panyoyai, N., Bannikova, A., Small, D. M., & Kasapis, S. (2015). Controlled release of thiamin in a glassy κ-carrageenan/glucose syrup matrix. *Carbohydrate Polymers, 115*, 723–731.
Paramita, V. D., Bannikova, A., & Kasapis, S. (2015). Release mechanism of omega-3 fatty acid in κ-carrageenan/polydextrose undergoing glass transition. *Carbohydrate Polymers, 126*, 141–149.
Pataca, L. C., Neto, W. B., Marcucci, M. C., & Poppi, R. J. (2007). Determination of apparent reducing sugars, moisture and acidity in honey by attenuated total reflectance-Fourier transform infrared spectrometry. *Talanta, 71*, 1926–1931.
Roos, Y., & Karel, M. (1991). Phase transitions of mixtures of amorphous polysaccharides and sugars. *Biotechnology Progress, 7*, 49–53.
Roos, Y. H. (2010). Glass transition temperature and its relevance in food processing. *Annual Review of Food Science and Technology, 1*, 469–496.
Santivarangkna, C., Aschenbrenner, M., Kulozik, U., & Foerst, P. (2011). Role of glassy state on stabilities of freeze-dried probiotics. *Journal of Food Science, 76*, 152–156.
Saxena, S., Gautam, S., & Sharma, A. (2010). Physical, biochemical and antioxidant properties of some Indian honeys. *Food Chemistry, 118*, 391–397.
Singleton, V. L., Orthofer, R., & Lamuela-Raventós, R. M. (1999). Analysis of total phenols and other oxidation substrates and antioxidants by means of folin-ciocalteu reagent. *Methods in Enzymology, 299*, 152–178.
Tewari, J., & Irudayaraj, J. (2004). Quantification of saccharides in multiple floral honeys using Fourier transform infrared microattenuated total reflectance spectroscopy. *Journal of Agricultural and Food Chemistry, 52*, 3237–3243.
Upadhyay, A. K., Chacko, A. R., Gandhimathi, A., Ghosh, P., Harini, K., Joseph, A. P., & Sowdhamini, R. (2015). Genome sequencing of herb Tulsi (*Ocimum tenuiflorum*) unravels key genes behind its strong medicinal properties. *BMC Plant Biology, 15*, 212.